Axial gain resolution in optical sectioning fluorescence microscopy by shaded-ring filters

M. Martínez-Corral, C. Ibáñez-López and G. Saavedra

Departamento de Óptica, Universidad de Valencia, 46100 Burjassot, Spain
manuel.martinez@uv.es, cristina.ibanez@uv.es, genaro.saavedra@uv.es

M. T. Caballero

Departamento de Óptica, Universidad de Alicante, P. O. Box 99, Alicante, Spain
mt.caballero@ua.es

Abstract: We present a new family of pupil masks to control the axial component of the intensity distribution in the focal region of tightly focused light fields. The filters, which consist of a circular clear pupil with a single shaded ring, allow to control the width of the central lobe of the axial spot together with the residual sidelobes energy. The filters can be applied to improve the optical sectioning capacity of different scanning microscopes.

OCIS codes: (350.5730) Resolution; (180.2520) Fluorescence Microscopy; (170.1790) Confocal Microscopy.

References and links

1. J. Pawley (ed.), *Handbook of Biological Confocal Microscopy* (Plenun, New York, 1995).
2. A. Diaspro (ed.) *Confocal and Two-Photon Microscopy. Foundations, Applications and Advances* (Wiley, New York, 2001).
3. C. M. Blanca, J. Bewersdorf and S. W. Hell, "Single sharp spot in fluorescence microscopy of two opposing lenses," Appl. Phys. Lett. **79**, 2321-2323 (2001)
4. T. A. Klar, E. Engel and S. W. Hell, "Breaking Abbe's diffraction resolution limit in fluorescence microscopy with stimulated emission depletion beams of various shapes", Phys. Rev. E **64**: 066613, 1-9 (2001).
5. M. A. A. Neil, R. Juskaitis, T. Wilson, Z. J. Laczik and V. Sarafis, "Optimized pupil-plane filters for confocal microscope point-spread function engineering," Opt. Lett. **25**, 245-247 (2000).
6. Z. Ding, G. Wang, M. Gu, Z. Wang and Z. Fan, "Superresolution with an apodization film in a confocal setup," Appl. Opt. **36**, 360-363 (1997).
7. C. J. R. Sheppard, "Binary optics and confocal imaging," Opt. Lett. **24**, 505-506 (1999).
8. M. Martínez-Corral, M. T. Caballero, E. Stelzer and J. Swoger, "Tailoring the axial shape of the PSF using the Toraldo concept," Opt. Express **10**, 98-103 (2002). www.opticsexpress.org/abstract.cfm?URI=OPEX-10-1-98
9. G. Boyer, "New class of axially apodizing filters for confocal scanning microscopy," J. Opt. Soc. Am. A **19**, 584-589 (2002).
10. G. Boyer and V. Sarafis, "Two pinhole superresolution using spatial filters," Optik **112**, 177-179 (2001).
11. C. M. Blanca and S. W. Hell, "Axial superresolution with ultrahigh aperture lenses," Opt. Express **10**, 893-898 (2002). www.opticsexpress.org/abstract.cfm?URI=OPEX-10-17-893
12. B. Richards and E. Wolf, "Electromagnetic diffraction in optical systems. II. Structure of the image field in an aplanatic system," Proc. Roy. Soc. (London) A **253**, 358-379 (1959).
13. P. D. Higdon, P. Török and T. Wilson, "Imaging properties of high aperture multiphoton fluorescence scanning optical microscopes," J. Microsc. **193**, 127-141 (1998).
14. C. J. R. Sheppard, "High apertured beams," J. Opt. Soc. Am. A **18**, 1579-1587 (2001).
15. K. Bahlman and S. W. Hell, "Electric field depolarization in high aperture focusing with emphasis on annular apertures," J. Microsc. **200**, 59-67 (2000).
16. M. A. A. Neil, F. Massoumian, R. Juskaitis and T. Wilson, "A method for the generation of arbitrary complex vector wavefronts," Opt. Lett. **27**, 1929-1931 (2002).
17. P. Török and F. J. Kao (eds.) *Optical Imaging and Microscopy: Techniques and Advanced Systems*, (Springer, Heidelberg, 2003).
18. J. W. M. Chon, X. Gan and M. Gu, "Splitting of the focal spot of a high-numerical objective in free space," Appl. Phys. Lett. **81**, 1576-1579 (2002).
19. I. Akduman, U. Brand, J. Grochmalicki, G. Hester, R. Pike and M. Bertero, "Superresolving masks for incoherent high-NA scanning microscopy in three dimensions," J. Opt. Soc. Am. A **15**, 2275-2287 (1998).

#2615 - $15.00 US Received June 19, 2003; Revised July 17, 2003

20. D. M. de Juana, J. E. Oti, V. F. Canales and M. P. Cagigal, “Design of superresolving continuous phase filters,” Opt. Lett. **28**, 607-609 (2003).
21. S. Mezouari and A. R. Harvey, “Phase pupil functions for reduction of defocus and spherical aberration,” Opt. Lett. **28**, 771-773 (2003).
22. H. Liu, Y. Yan, D. Yi and G. Jin, “Design of three-dimensional superresolution filters and limits of axial optical superresolution,” Appl. Opt. **42**, 1463-1476 (2003).
23. G. Toraldo di Francia, "Nuovo pupille superresolventi," Atti Fond. Giorgio Ronchi **7**, 366-372 (1952).
24. J. Campos, J. C. Escalera, C. J. R. Sheppard and M. J. Yzuel, “Axially invariant pupil filters,” J. Mod. Opt. **47**, 57-68 (2000).
25. S. Grill and E. H. K. Stelzer, "Method to calculate lateral and axial gain factors of optical setups with a large solid angle," J. Opt. Soc. Am. A **16**, 2658-2665 (1999).
26. C. J. R. Sheppard, "Leaky annular pupils for improved axial imaging," Optik **99**, 32-34 (1995).
27. C. J. R. Sheppard and P. Török, “An electromagnetic theory of imaging in fluorescence microscopy, and imaging in polarization fluorescence microscopy,” Bioimaging **5**, 205-218 (1997).
28. D. Ganic, J. W. M. Chon and M. Gu, “Effect of numerical aperture on the splitting feature near phase singularities of focused waves,” Appl. Phys. Lett. **82**, 1527-1528 (2003).
29. M. Martínez-Corral, L. Muñoz-Escrivá, M. Kowalczyk and T. Cichocki, "One-dimensional iterative algorithm for three-dimensional point-spread function engineering," Opt. Lett. **26**, 1861-1863 (2001).

1. Introduction

The use of wide-field optical microscopes to image three-dimensional (3D) biological or medical samples have an important drawback: an image focused at a certain depth in the specimen contains blurred information from the entire one. To overcome this problem, the use of optical sectioning fluorescence techniques was proposed. We can cite single-photon fluorescence confocal scanning microscopes (CSM’s), in which the monochromatic light from a point source is focused onto a small region of a 3D fluorescent sample by a high-NA objective. The fluorescent light emitted by the sample is collected by the same objective, passes through a pinhole located at the conjugate plane, and is finally detected. The 3D image is reconstructed with a computer from the intensity values acquired by 3D scanning the sample [1]. The main feature of CSM’s is their uncommon depth discrimination capacity. However, the axial resolution of CSM’s is much poorer than their lateral resolution. This fact leads to an anisotropic 3D imaging quality. We can also cite the two-photon excitation (TPE) scanning microscopy, which is a nonlinear optical technique that constitutes one of the most promising areas in biological and medical imaging at microscopic level [2]. This technique relies on the simultaneous absorption of two photons, following which a single fluorescence photon is emitted. The excitation wavelength is typically twice than in the single-photon case. The fluorescence intensity is now proportional to the square of the illumination intensity. Thus, TPE microscopes have the ability of strongly limiting the effective excitation region and inherently possess optical sectioning capacity. The overall fluorescent light is collected and detected, and the final image is synthesized from the 3D sampling of the object. Also here the difference between axial and lateral resolutions results in 3D images with anisotropic quality.

Several attempts have been done to improve the axial resolution of optical sectioning microscopes. We can cite the 4Pi-confocal microscopes, in which two opposing high-NA objectives are used to coherently illuminate the fluorescence probe and therefore to create a very narrow focal spot [3]. The stimulated emission depletion (STED) microscopy breaks the diffraction barrier by inhibiting fluorescence molecules at the outer region of a scanning excitation spot in a saturated manner [4]. These techniques have revealed to be extremely efficient in improving the axial resolution. Other less efficient techniques are also of interest due to their simplicity. This is the case of the so-called point-spread-function (PSF) engineering, which with a minimum modification of microscopes architecture significantly improve their performance. In the past few years the use of purely-absorbing or complex-transmittance pupils has been proposed in confocal scanning microscopes [5-10] or TPE scanning microscopes [11]. However, the filters can severely reduce the focused-light efficiency in fluorescence microscopy, since they produce an important increment of the sidelobes energy. To avoid this fault, in this paper we design a new family of pupil filters,

#2615 - $15.00 US Received June 19, 2003; Revised July 17, 2003

which have the ability to compress the main peak of the axial spot, but attenuating the sidelobes energy.

2. The axial PSF of high-NA focusing systems

Let us consider the electric field distribution in the focal region of an aberration-free high-NA focusing system illuminated by a monochromatic, linearly polarized wave-front of wavelength λ. According to Richards and Wolf [12], for rotationally symmetric systems this field is

$$\mathbf{E}(r,z,\varphi;\lambda)=\left[I_0(r,z;\lambda)+I_2(r,z;\lambda)\cos\varphi\right]\mathbf{i}+I_2(r,z;\lambda)sin2\varphi\,\mathbf{j}-2I_1(r,z;\lambda)\cos\varphi\mathbf{k}\ , \qquad (1)$$

where $I_{0,1,2}$ are integrals over the aperture angle θ at the exit pupil plane as seen from the focus, and φ represents the angle between the polarization direction of the incident field (assumed *x*-direction) and the observation meridian plane. As clear from Eq. (1), strong focalization can produce a significant change in the beam polarization. This phenomenon, known as *depolarization*, has attracted the interest important research efforts in the past few years [13-18]. A matter of special interest is the study of the structure of the axial component of the field. If we set $r=0$ in Eq. (1) we find that

$$\mathbf{E}(r=0,z,\varphi;\lambda)=\mathbf{i}\,I_0(r=0,z;\lambda)=\mathbf{i}\int_0^{\alpha}P(\theta)(1+\cos\theta)\exp\left(i2\pi n\frac{\cos\theta}{\lambda}z\right)\sin\theta\,d\theta\ , \qquad (2)$$

$P(\theta)$ accounting for the amplitude transmittance at the exit pupil, α being the maximum value of the aperture angle θ and n standing for the refraction index. Note that along the optical axis the field no longer suffers the depolarization process. This fact permits to analyze the axial PSF in a quite simple way, after performing the following nonlinear mapping

$$\zeta=\frac{\cos\theta-\cos\alpha}{1-\cos\alpha}-0.5\quad;\qquad Q(\zeta)=(1+\cos\theta)P(\theta)\ . \qquad (3)$$

Now the axial amplitude can be rewritten as

$$E(r=0,z,\varphi;\lambda)=E_o(z_N)=(1-\cos\alpha)\exp\left(i\pi\frac{1+\cos\alpha}{1-\cos\alpha}z_N\right)\int_{-0.5}^{0.5}Q(\zeta)\exp(i2\pi\zeta\,z_N)\,d\zeta\ , \qquad (4)$$

where $z_N=n(1-\cos\alpha)z/\lambda$. Since the field $\mathbf{E}(r=0,z,\varphi;\lambda)$ is linearly polarized along the *x*-direction, we have omitted the explicit reference to its vectorial character in Eq. (4). Such an equation indicates that the axial amplitude is proportional to the 1D Fourier transform of the nonlinearly mapped transmittance. To obtain a given axial distribution it is necessary a function $Q(\zeta)$ whose 1D Fourier transform closely approximates the desired form. A classical approach to this aim is the design of phase-only filters by different algorithms [19-21] or by techniques [8,22] based on the Toraldo concept [23]. It is commonly assumed that, since they produce no light losses, the phase-only filters give the optimum solution. However, such filters usually produces huge sidelobes and, consequently, rather poor light efficiency. Due to this fact, this paper is devoted to the design of optima purely-absorbing pupil filters.

3. Design of optima purely-absorbing axially-superresolving filters

A procedure equivalent to that reported in Ref. [5] allows to find that the width of the axial intensity distribution is proportional to the inverse of the standard deviation, σ_a, of $Q(\zeta)$. Then, the axial gain in resolution for tightly focused beams can be defined as $G_A=\sigma_a/\sigma_c$, where subscript c refers to the nonapodized circular aperture. The concept of nonparaxial gain in axial resolution was already defined in Ref. [24], and applied to calculate the performance of several filters [25], but, to the best of our knowledge, it was never used as a design tool.

To obtain axial superresolution it is necessary a filter such that $\sigma_a>\sigma_c$. Thus, the value of $Q(\zeta)$ in the vicinity of $\zeta=-0.5$ and $\zeta=+0.5$ should be higher than at $\zeta=0$. The simplest solution

#2615 - $15.00 US Received June 19, 2003; Revised July 17, 2003

is a binary filter such that $Q(\zeta)$ consists of two equal-width rectangles (Fig. 1(a) green curve). These filters, commonly known as dark-ring (DR) filters, have shown to be very useful in bright-field confocal microscopy [5], and also in two-photon confocal microscopy [11,3]. However, since they produce very high axial sidelobes, they are not too useful in CSM or in TPE microscopy. In the first case the high axial sidelobes can produce photo-bleaching of the specimen in parts of it not in focus. In the second case, the sidelobes are not removed by any detection pinhole, and then the improvement in axial resolution is not effective.

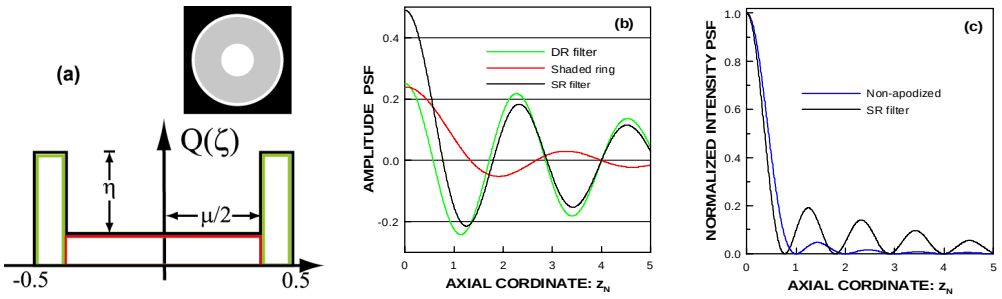

Fig. 1. (a) Mapped transmittance of a SR filter (black curve). The SR filter is composed by a DR filter (green curve) and a shaded ring (red curve); (b) Amplitude PSF of the SR filter (black curve) which is calculated as the sum of two amplitude PSF's: the one of the DR filter and that of the shaded ring; (c) Intensity PSF of the SR filter, as compared with the PSF of the nonapodized objective. The parameters for the calculation were μ=0.75, η=0.68.

We propose to substitute the dark ring for an adequate shaded ring. The performance of shaded-ring (SR) filters is illustrated in Fig. 1. The contribution of the shaded ring to the axial pattern is significant only in the central part. Then, the axial PSF produced by the SR filter (black curve) exhibits a central lobe that is much higher than the one produced by the DR filter (green curve), whereas the sidelobes height remains almost invariant. The SR filters can be understood as members of a more general class of filters known as leaky filters [26]. Calculation of the axial gain for SR filters gives

$$G_A = \sqrt{\left(1-\eta\mu^3\right)/\left(1-\eta\mu\right)}\,, \tag{5}$$

where the parameters η and μ are described in Fig. 1(a). Note that all pairs (η,μ) fulfilling Eq. (5) correspond to filters with the same gain but different sidelobes energy. Any pair $(\eta=1,\mu)$ corresponds to a DR filter, considered now as a member of the SR-filters family.

4. Application to scanning microscopes

Due to their scanning nature, single-photon fluorescence CSM's are 3D linear and shift-invariant (LSI) systems. If we consider that, in an optimum case, the objectives are aberration free, used in the design conditions, and that the refraction index of the immersion medium is that of the specimen, the 3D intensity PSF can be calculated as

$$\begin{aligned}\mathrm{PSF}(r,z,\varphi;\lambda_{ill},\lambda_{det}) &= \mathrm{PSF}_{ill}(r,z,\varphi;\lambda_{ill})\,\mathrm{PSF}_{det}(r,z;\lambda_{ill}/\varepsilon) = \\ &= \left|\mathbf{E}_{ill}(r,z,\varphi;\lambda_{ill})\right|^2 \left\langle \left|\mathbf{E}_{det}(r,z,\varphi;\lambda_{ill}/\varepsilon)\right|^2 \right\rangle_{\varphi},\end{aligned} \tag{6}$$

where linearly x-polarized illumination is assumed, $\varepsilon=\lambda_{ill}/\lambda_{det}$ represents the ratio between the excitation and fluorescence wavelengths. $\mathbf{E}_{ill}$ is accurately described by Eq. (1), which is only good approximation for field in detection [27]. The angular brackets in Eq. (6) stand for the φ-average process associated with the usual assumption of random polarization for the fluorescent light. Note that confocal PSF is a non-radially symmetric function that explicitly depends on the angle between the illumination polarization and the observation meridian plane.

We propose to narrow the confocal PSF by use of SR filters in the illumination arm of the

#2615 - $15.00 US Received June 19, 2003; Revised July 17, 2003

microscope. There are two basic reasons that advise against the use of these filters in the detection arm. First, due to the pinholed detection, the light efficiency of collecting system is very poor and fluorescent light losses should be avoided. The second and most important reason results from the fact that, due to the mismatch between illumination and collection wavelengths, the collection PSF is about 25% wider than the illumination PSF. Then, narrowing the collection PSF would have only an insignificant influence onto the confocal PSF width.

Among the family of SR filters with the same value for the axial gain, we will select the one that maximizes the focused-light efficiency, understood as the ratio between the central-lobe energy and the overall diffracted energy. In other words, the one that minimizes the sidelobes to peak ratio (*SLPR*), defined as

$$SLPR = \int_{z_p}^{+\infty} \left|\mathbf{E}_{ill}(r=0,z,\varphi;\lambda_{ill})\right|^2 dz \Big/ \int_0^{z_p} \left|\mathbf{E}_{ill}(r=0,z,\varphi;\lambda_{ill})\right|^2 dz \ , \qquad (7)$$

z_p being the coordinate of the first zero-intensity axial point. In Fig. 2(a) we have drawn several curves with constant value for G_A but varying *SLPR*. Any point at the curves corresponds to a different (η,μ) pair. As mentioned above, the left-end point at any curve corresponds to the DR filter. For our numerical experiment we selected G_A=1.20. The minimum of the curve corresponds to the SR filter μ=0.67 and η=0.66. In terms of the *SLPR* the selected SR filter is 25% better than the DR filter. We also show the 3D PSF of a confocal instrument with two circular pupils (Fig. 2(b)) and with the SR filter in the illumination (Fig. 2(c)). It is obtained an important improvement (12.0% in terms of the *FWHM*) in axial resolution, and only a small worsening (1.8%) in lateral resolution.

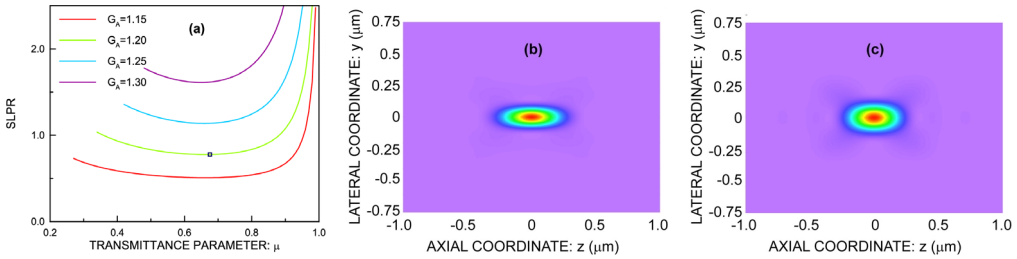

Fig. 2. (a) *SLPR* values for families of SR filters with the same axial gain; (b) Numerically evaluated 3D PSF (pseudo-colored) of a confocal instrument with two circular pupils; (c) Same as (b) but with the selected SR filter in illumination. The parameters for the calculation where: $\varphi=\pi/2$, λ_{ill}=350 nm, λ_{det}=440 nm (Coumarin 400) and *NA*=1.2 (water).

The optical-sectioning capacity of an imaging system can be better evaluated in terms of the *z*-response, which is defined as the 1D image acquired by axially scanning a very thin fluorescent layer. Calculations not shown demonstrate that the SR filter narrows the *z*-response by 12.5%. As a meter of the enhancement obtained with our method we point out that the same narrowness would be obtained by using an objective with circular aperture and *NA*=1.246, which is not commercially available.

Let us consider now the case of TPE scanning microscopes in which the overall fluorescent light is collected without pinhole. In such systems the fluorescence intensity is proportional to the square of the illumination intensity. TPE microscopes have the ability of strongly limiting the excitation region and inherently possess optical sectioning capacity even in the absence of pinholed detection. When no photobleaching affects the sample and no saturation effects occur, TPE microscopes are 3D LSI systems whose PSF is given by

$$\mathrm{PSF}_{2p}(r,z,\varphi;\lambda_{ill}) = \left|\mathbf{E}_{ill}(r,z,\varphi;\lambda_{ill})\right|^4 . \qquad (8)$$

Note that Eq. (8) does no take into account the spectral width of the short pulsed beams commonly used in TPE, since it refers to a single wavelength λ_{ill}. A more accurate formulation

#2615 - $15.00 US
Received June 19, 2003; Revised July 17, 2003

should express the PSF_{2p} as an incoherent weighted superposition of the spectral components of the beam [28]. However, since the transmission function of SR filters is not wavelength dependent, the only difference between the spectral components of the PSF_{2p} is a scale effect that affects in similar way the apodized and the nonapodized setup. Therefore, to compare the performance of SR filters with the clear pupil we will use the monochromatic-like Eq. (8) in our calculations. Following this reasoning, it can be probed that the axial gain G_A is also given in this case by Eq. (5). The merit function to be optimized now is

$$SLPR_{2p} = \int_{z_p}^{+\infty} \left|\mathbf{E}_{ill}(r=0,z,\varphi;\lambda_{ill})\right|^4 dz \Big/ \int_0^{z_p} \left|\mathbf{E}_{ill}(r=0,z,\varphi;\lambda_{ill})\right|^4 dz \quad . \tag{9}$$

In Fig. 3(a) we draw several curves with constant value for G_A but varying $SLPR_{2p}$. Note that the achievable values for $SLPR_{2p}$ are now much better than in the CSM case. This allows us to select a higher value for the gain. For the numerical experiment we selected the curve G_A=1.25. The SR filter that minimizes the merit function is: μ=0.88, η=0.81. For this optimal filter $SLPR_{2p}$=0.16, which is 73% smaller than the corresponding to the DR filter with the same axial gain. In Fig. 3(b) we compare the PSF_{2p} with the corresponding to the non-apodized case. The benefits of using SR filters are more appreciable in TPE microscopy than in the previous case. Specifically, the axial resolution is improved by a 20%, whereas the transverse resolution is worsened only by a 2.9%. It is apparent that the use of SR filters produces an important improvement in axial resolution at the expense of only small worsening of focused-light efficiency (calculated as 100 $(1+SLPR_{2p})^{-1}$), which downs from 99% in the nonapodized case, to 86% in case of the SR filter (62% for the DR filter).

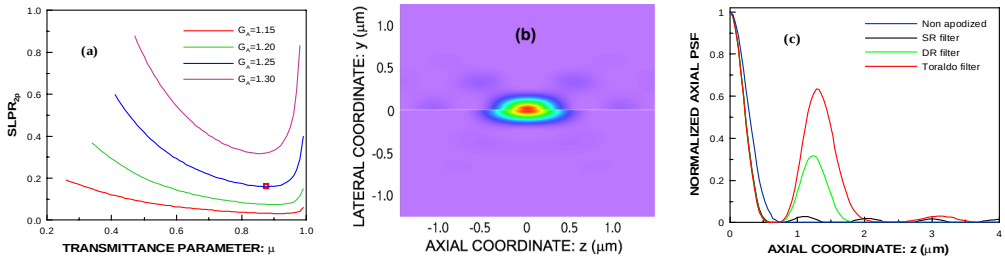

Fig. 3. (a) $SLPR_{2p}$ values for families of SR filters with the same axial gain; (b) Numerically evaluated 3D PSF (pseudo-colored) of a TPE scanning microscope with circular pupil (bottom) or with the selected SR filter (top); (c) Comparison of axial PSF's corresponding to different kind of filters. The parameters for the calculation where: $\varphi=\pi/2$, λ_{ill}=700 nm, and NA=1.2.

Let us emphasize that in the case of TPE microscopy the simple insertion of a pupil mask in the illumination path can yield important benefits in imaging quality. Since binary filters have shown to efficiently work in TPE setups [3,11], we estimate that the SR filters could be easily implemented by photolithography making use of digital halftoning techniques [29].

5. Conclusions

In summary we have presented a new set of annular filters specifically designed to improve the axial resolution of optical-sectioning fluorescence scanning microscopes. The SR filters consist of a shaded ring with adequate width and light transmittance. The insertion of such filters in the illumination pupil of the microscope produces an important improvement of optical sectioning capacity. The numerical experiments show that the proposed filters are useful in both single-photon CSM and TPE scanning microscopy.

Acknowledgements

We would like to express our gratitude to two anonymous reviewers, whose comments and suggestions helped to improve the quality of the paper. This work was funded by the Plan nacional I+D+I (grant DPI2000-0774), Ministerio de Ciencia y Tecnología, Spain. C. Ibáñez-López gratefully acknowledges the financial support from the same institution.